COMPOSITES 2006 Convention and Trade Show
American Composites Manufacturers Association
October 18-20, 2006
St. Louis, MO USA

Pultruded FRP Plank as Formwork and Reinforcement for Concrete Structures

by

Lawrence Bank
Michael Oliva
Han-Ug Bae
Jeffrey Barker

University of Wisconsin, Madison, WI

Seung-Woon Yoo

Kwandong University, Kangwon, Korea

Abstract

A feasibility study in which a pultruded fiber reinforced polymer (FRP) plank was used as the both formwork and the tensile reinforcement for a concrete structural member is described in this paper. The study was motivated by the desire to use the FRP plank as a stay-in-place form and reinforcement for a new bridge that is currently being designed in Wisconsin and will be constructed in early 2007. For the FRP plank and the concrete to act as a "composite" structural member a satisfactory bond at the interface between the smooth surface of the pultruded plank and the concrete must be developed. To achieve this interface, stone aggregates of different sizes were bonded to the surface of the pultruded FRP plank. Two kinds of aggregate, gravel and sand, were bonded to the pultruded FRP plank using a commercially available epoxy system. Concrete beams of different lengths were fabricated using a commercially available pultruded FRP plank. No additional flexural or shear reinforcement was provided in the beams. Two of the beams were used as control specimens. One control did not have any aggregate bonded to the FRP plank and the other control had internal steel reinforcing bars instead of the FRP plank. The beams were loaded by central patch load to their ultimate capacity. The experimental results were compared to current ACI 318 and ACI 440 code predictions. Depending on the length of the beam, shear or flexural failures occurred, which demonstrated satisfactory bond between the FRP plank and the concrete. The ultimate capacity of the aggregate coated FRP plank specimens was higher than that of the control specimens. This study demonstrates that the FRP plank has the potential to serve as formwork and as tensile reinforcement for appropriately sized concrete beams.

Introduction

In the last decade there have been numerous applications of FRP composite materials as internal reinforcements (known as "rebars") for concrete structures (ACI, 2006). FRP reinforcing materials are generally used to prevent corrosion problems in reinforced concrete structures that plague conventional steel reinforced concrete structures. In addition there have been widespread applications of bonded FRP materials for repairing or strengthening concrete structures. The use of hybrid FRP/concrete members with a dual purpose of both formwork and reinforcement, has been considered in some studies and has been applied in a number of bridge decks (Deskovic et al 1995, Hall and Mottram 1998, Hullat et al, 2003, Dieter et al. 2004, Matta et al, 2005, Cheng et al. 2005 and Berg et al 2006). A combined formwork and reinforcement system can facilitate rapid construction of concrete members since no conventional formwork is needed, which requires time consuming assembly and dismantling. In order for a smooth pultruded FRP plank to act compositely with the concrete the surface of the FRP plank needs to be treated to increase its bond properties.

In this study, an inverted portion of a commercially available FRP plank having integral T-shaped ribs, shown in Fig. 1a, was used as the formwork and the reinforcement for the concrete. The FRP plank is produced in 12 and 24 inch widths and is used in walkway or flooring applications with the flat side facing up and has a smooth inner surface. (Silica sand grit is often applied to the flat surface of the plank to create a non-slip walking surface). Two types of stone aggregate, sand and gravel, were bonded to the inner flat surface of the plank to improve the bond between the concrete and the FRP plank. The aggregate was bonded with epoxy to the FRP plank, which was cured, prior to the placement of the concrete. The feasibility of using this system was investigated experimentally using beams of different lengths that were tested in three point bending. The test results from the FRP plank specimens were compared to code predictions and to the results obtained from the control specimens.

Fabrication of Specimens

Five 8" wide by 7" deep beams (specimens 1-5) with different lengths (three beams with a 3' 7" span and two beams with a 6' span) were fabricated using the aggregate coated FRP plank as the bottom formwork for the concrete (see Table 1 for details). No other tensile or shear reinforcement was used in the beams. Longitudinal tension tests were conducted on the FRP plank material yielding a longitudinal tensile strength, σ_L = 69,800 psi and a longitudinal modulus of elasticity, E_L = 3.9×10^6 psi (Ringelstetter, 2006). Fig. 1b shows the approximate cross sectional dimensions of a two-legged portion of the FRP plank that was used in the tests. The 8” wide portion, shown in Fig. 1b, was cut from the center portion of the 12” wide FRP plank, shown in Fig. 1a, to produce a representative unit width element of the FRP plank reinforced beam. Fig. 2 shows the dimensions of the specimens.

The first step of the fabrication was to cut the FRP planks to the appropriate dimensions. Thereafter, a construction-grade epoxy was spread on top (inner) surface of the plank. Epoxy was only placed between the ribs of the plank on the bottom horizontal surface. No epoxy or aggregate was bonded to the protruding vertical ribs on either the flanges or the webs of the ribs. The epoxy was placed directly on the as-received pultruded material which was not roughened or sanded. The gravel or sand was scattered on the wet epoxy using a perforated bucket to cover approximately 30% of the total area. Sizes of the aggregates were 1/8”~1/4” for the gravel and 1/16”~1/10” for the sand. Fig. 3 shows the aggregate coated FRP planks. Plywood forms were then constructed around the FRP planks to form the sides of the beam specimens which were then cast using concrete from a local ready-mixed commercial concrete vendor. A Wisconsin DOT Grade D, Size 1 (3/4” max. aggregate size) concrete design mix, having a 28-day target compressive strength of 4,000 psi, was specified for all test specimens.

Two 8” wide by 7” deep beams (specimen C1 and C2) were also fabricated as control specimens for comparison. One of the control specimens, C1, having a length of 3’ 7” was fabricated using the FRP plank as formwork, but no aggregate was bonded on top of the FRP plank. This control specimen served as the control for FRP plank specimens 1-3 and was intended to show the difference between the specimens with and without the aggregate when tested over short spans that would be shear dominated. The other control specimen, C2, was a conventional steel reinforced concrete beam with a 6’ span, with no shear reinforcement and no FRP plank. The beam was reinforced with three # 3 Grade 60 steel rebars (60 ksi nominal yield strength) with 1-1/2” of clear bottom cover. This reinforcement quantity was the same as that needed for the bottom transverse reinforcement in a steel reinforced bridge deck with a 3 ft clear span between girders (the edge of girder flange to the edge of adjacent girder flange). The choice of the 3 ft clear span for the steel reinforcement was made since the clear span between the girder flanges of the new bridge to be constructed in Wisconsin and for which this study was conducted is 3 ft. This control specimen was used to compare the performance of the FRP plank beam to that of a conventional steel reinforced beam of a longer span that would be flexurally dominated. The purpose of this investigation was to see if the aggregate coated FRP plank could serve as the positive moment reinforcement for the bridge deck, both from a strength (i.e., capacity) and a serviceability (i.e., crack control) perspective. Details of all the fabricated beams including control specimens are summarized in the Table 1.

Experimental setup and instrumentation

The beam test specimens were placed on two steel bearing plates 2 inches wide in a simply supported configuration. The center-to-center spacing of the bearing plates was either 3’ 7” (specimens 1-3 and C1) or 6’ (specimens 4-5 and C2). A steel roller was place under the center of each bearing plate to allow rotation at the supports.

Deflections were recorded with linear variable differential transformers (LVDTs) at the center of the specimen. A load cell on the head of the hydraulic actuator measured loads during the experiments. Longitudinal strains of the FRP plank and the concrete were measured using electrical resistance strain gauges. The strain gauges were offset 3-1/2” in the longitudinal direction from the center of the beam to avoid interfering with load head. Fig. 4 shows the typical experimental instrumentation used for the testing.

The load was applied at the center of the specimen in a three point bend test configuration by a hydraulic actuator under manual displacement control. A 3 inch wide steel plate was placed at the bottom of the loading head. Gypsum cement was cast between the loaded top surface of the specimen and the steel plate to transfer load uniformly along the center line of the specimen. Figs. 5 and 6 show the test setup for the specimens 1 and 4, respectively.

Experimental Results

Comparison criteria

Three criteria were selected to investigate the composite action between the FRP plank and the concrete during the experiments. The first criterion was the initial cracking load of the specimen. This was obtained from observations in the changes of the strain gauge readings and the deflection readings during the test. The second criterion was the distribution of flexural cracks. Flexural (and shear) cracks were marked and counted during the experiments. It was expected that the bond between the FRP plank and the concrete provided by the aggregate coating would prevent slip between the FRP and the concrete and as a result closely spaced flexural cracks having small widths would occur as opposed to a few wide and sparsely-spaced cracks. The third criterion was the capacity of the specimen and its failure mode. Three failure modes were considered. These were a flexural mode, a shear mode and the hybrid flexural/shear (combined) mode.

Initial cracking capacity

The initial flexural cracking load was identified by observing the change in slope of the load-strain curves. The load obtained from the strain gages was typically less than the cracking load obtained by visual observation of the occurrence of the first flexural crack. The initial cracking loads and the strains at the initial cracking loads are shown in Table 2. All the initial cracks were observed near the center of the specimens. The loads obtained from each test were converted to give the cracking moment and normalized with respect to a 4,000 psi compressive strength concrete to account for the differences in the strengths of the concrete. The normalization was performed by multiplying the calculated moment by $\sqrt{\frac{f_c'}{4{,}000}}$.

The beams (specimens 1-5) with the aggregate coated FRP planks showed higher initial cracking capacities compared to the control specimen reinforced by the FRP plank with the smooth surface (specimen C1) and compared to the specimen with the steel reinforcing bars (specimen C2). This indicates that coated FRP plank can produce an increase in the initial cracking moment capacity of a concrete beam, which may be a serviceability benefit for a reinforced concrete section, particularly a bridge deck. The beams with the sand coated FRP plank (specimen 2 and 3) showed higher initial cracking capacity than the specimen with the gravel coated FRP plank (specimen 1), indicating that sand coating provides a more even interface than the gravel in the interface region.

Distribution of flexural cracks

Current design codes allow a concrete structure to crack under service loads, however, the width of the cracks is typically limited to the prescribed value. The aggregate coating may have ability to better distribute cracks which would lead to narrower crack widths. This is provided that no slip or very little slip occurs at the interface between the FRP plank and the concrete. A comparison of numbers of cracks was, therefore, an important evaluation criterion in this study.

The number of the flexural cracks was counted after the failure of each specimen (Table 2). In the short beams, 9-11 small flexural cracks occurred in the aggregate coated case (specimens 1-3) and 3 large cracks occurred in the case without the aggregate coating (specimen C1). This clearly shows that aggregate coating provides a mechanism to distribute the cracks and to transfer bond stresses at the interface between the FRP plank and the concrete. The gravel coated beam (specimen 1) showed slightly better performance than the sand coated beams (specimen 2-3). This was also confirmed by crack width measurements. In the long beams (specimens 4 and 5), 22-29 flexural cracks were measured. This was similar to that of the steel control beam (specimen C2) as shown in Table 2. This demonstrates that the aggregate coated FRP plank can serve as an effective tensile reinforcement and can distribute flexural cracks in a similar manner to internal steel reinforcements.

Capacities and failure modes

The specimens reinforced by the aggregate coated FRP planks failed in a number of different modes. The failure modes were shear failure for specimens 1-3, flexural failure with a significant slip at the interface of the FRP plank and the concrete for specimen C1, hybrid flexural/shear failure for specimens 4-5 and flexural failure with yielding of the steel rebars followed by concrete crushing for specimen C2. Capacities of the tested specimens are listed in Table 2. Figs. 7-8 show the specimens after the test, Figs. 9-10 show the load vs. defection curve for the tested specimens and Figs. 11-12 show the load vs. strain curve for the tested spciemens. As can be seen from Table 2, the control specimens showed less capacity than the aggregate coated FRP plank specimens.

Distributed flexural cracks occurred during the initial loading stages of specimens 1-3. As the load approached the maximum value, a number of the flexural cracks developed into diagonal shear cracks. Finally a critical diagonal shear crack formed that lead to the beams failing in shear, as seen in Figs. 7(a) – (c). Partial debonding between the FRP plank and the concrete was observed at the midspan during the tests for all the beams. However, there was no evidence of any slip of the FRP plank from the concrete at the end of the beam following the shear failure of the specimens. The compressive and tensile strain levels recorded by the strain gauges (less than 0.001 for concrete in compression and 0.0045 for FRP in tension) are evidence that there was no concrete crushing or FRP tensile failure at the ultimate load.

The control specimen for the specimens 1-3 (specimen C1) failed in a flexural mode with a significant amount of slip between the FRP plank and the concrete as seen in Fig. 7 (d). When specimen C1 was loaded after reaching its first peak, it continued to resist additional load and a secondary peak was seen. This secondary peak seemed to be due to the tensile force provided by the FRP plank that was trapped under the supports, or may have been due to residual friction. The specimen was felt to have lost its composite action at the first load peak due to the previously noted significant slip. The first peak load was, therefore, selected as an ultimate capacity of this specimen. The load deflection curves of the 3' 7" beams are shown in Fig. 9.

Specimens 4-5 failed in a hybrid mode of shear and flexure at the failure load, after the occurrence of distributed flexural cracking. This failure mode was felt to have occurred since a significant diagonally crack developed simultaneously with visible concrete crushing near the loaded area, as seen in Figs. 8 (a) & (b). This can also be classified as a shear-compression failure. At failure the compressive strain level at the top surface of the concrete reached 0.003 which is generally accepted to the failure strain of concrete in compression. The control specimen (specimen C2) for specimens 4-5 failed in a flexural mode with yielding of steel reinforcement followed by crushing of concrete which is the typical failure mode of an under-reinforced steel reinforced beam, as seen in Fig. 8 (c). The ultimate capacity for the specimen C2 was 58~64% of specimens 4 and 5 and demonstrates that the aggregate coated FRP plank can be used as tensile reinforcement instead of the steel reinforcement for a beam designed to achieve the capacity of the steel reinforced beam. As can be seen from the load-deflection plot in Fig. 10 the deflection at failure in the steel reinforced beam is much larger than that of the FRP plank reinforced beam. However, the load at failure in the FRP plank beam is larger than that of the steel beam. This is a common situation in over-reinforced FRP beams (ACI, 2006).

Comparison of experiment to code prediction

Test results were compared to current ACI 318 and ACI 440 code predictions and listed in Table 3. The prediction of the capacities from the code equations were performed based on assumptions that FRP plank does not contribute on cracking resistance and there is full composite action between the FRP plank and the concrete. ACI 318 predictions for the cracking capacity were conservative except for the specimen C2. Compared to the experimental results, ACI 318 equations for shear capacity of the beams predicted better values than those of ACI 440. When using ACI 318 or ACI 440 for the calculation of the shear and flexural capacities of the FRP plank reinforced beams the resultant tensile force in the FRP was assumed to be applied at the centroid of the FRP section which was located at a height of 0.503 inches. The total area of the FRP plank in the 8 inch wide portion was 2.075 in^2. The design strength and the design modulus were taken as, f_{fu} = 69,800 psi and $E_f = 3.9 \times 10^6$ psi respectively (i.e., no environmental or resistance factors were used in the calculations and the average strength was assumed to be the guaranteed strength obtained from testing of the FRP). All the FRP plank beams were over-reinforced beams in flexure.

Conclusions

Experimental studies were performed to investigate if an aggregate coated FRP plank could serve as a tensile reinforcement for concrete beams. The results of the testing indicate that the aggregate coated FRP plank can serve as an alternative to conventional steel reinforcement. The aggregate coated FRP plank beams performed as well or better than the steel reinforcement in terms of initial cracking moment capacity, ability to distribute flexural cracks and ultimate load carrying capacity. The epoxy bonded aggregate coating at the surface of the FRP plank was essential to developing composite action. The use of the FRP plank without the surface treatment as a tensile reinforcement showed the significant slip between concrete and considerably less capacity during test. Sand and gravel aggregate were used in this study and both were found to be acceptable. Since it has been demonstrated that the aggregate coated FRP plank can be used as a tensile reinforcement, it can also be used as a stay-in-place form. This will lead to construction efficiency and may also produce a more durable bridge deck. Based on the results of this study an FRP plank stay-in-place form and reinforcement system will be used in the construction of a new bridge in Wisconsin in the coming year.

Acknowledgements

Funding for this project was provided by the Federal Highway Administration (FHWA) through the Innovative Bridge Research and Construction Program (IBRC) and by the Wisconsin Department of Transportation (WisDOT). Special thanks are due to Finn Hubbard and Scott Becker of WisDOT and to Strongwell for supplying FRP materials for the study.

References

ACI (2005), "Building Code Requirements for Structural concrete" ACI 318-05, American Concrete Institute, Farmington Hills, MI.

ACI (2006), "Guide for the Design and Construction of Structural Concrete Reinforced with FRP Bars," ACI 440.1R-06, American Concrete Institute, Farmington Hills, MI.

Berg, A.C., Bank, L.C., Oliva, M.G., and Russell, J.S. (2006), "Construction and cost analysis of an FRP reinforced concrete bridge deck," *Construction and Building Materials*, Vol. 20, pp. 515-526.

Cheng, L., Zhao, L., Karbhari, V.M., Hegemier, G.A., and Seible, F. (2005), "Assessment of a steel-free fiber reinforced polymer-composite modular bridge system," *Journal of Structural Engineering*, Vol. 131, No. 3, pp. 498-506.

Deskovic, N., Triantafillou, T.C., and Meier, U. (1995), "Innovative design of FRP combined with concrete: Short-term behavior," *Journal of Structural Engineering*, Vol. 121, No. 7, pp. 1069-1078.

Dieter, D.A., Dietsche, J.S., Bank, L.C., Oliva, M.G., and Russell, J.S. (2002), "Concrete bridge decks constructed with FRP stay-in-place forms and FRP grid reinforcing," Transportation Research Record No.1814, *Journal of the Transportation Research Board*, pp. 219-226.

Hall, J.E., and Mottram, J.T. (1998), "Combined FRP reinforcement and permanent formwork for concrete members," *Journal of Composites for Constructions*, Vol. 2, No. 2, pp. 78-86.

Hulatt, J., Holloway, L., and Thorne, A., (2003), "The use of advanced polymer composites to form an economic structural unit," *Construction and Building Materials*, Vol, 17, No, 1, pp. 55-68.

Matta, F., Galati, N., Nanni, A., Ringelstetter, T.E., Bank, L.C., and Oliva, M.G., (2005), "Pultruded grid and stay-in-place form panels for the rapid construction of bridge decks," *COMPOSITES 2005 Convention and Trade Show*, American Composites Manufacturers Association, September 28-30, Columbus, OH.

Ringelstetter, T.E., (2006), "Investigation of modular FRP grid reinforcing systems with integral stay in place form for concrete structures," MS Thesis, University of Wisconsin, Madaion.

Figure-1a 12 inch wide pultruded FRP plank

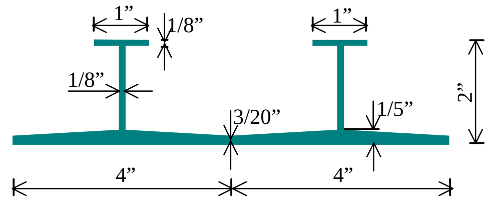

Figure-1b Approximate cross-sectional dimensions of potion of FRP plank used in test beams

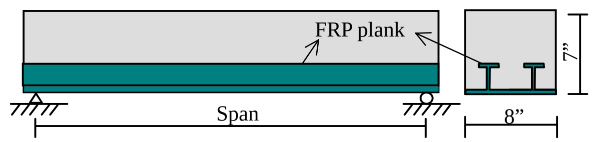

Figure-2 Dimension of fabricated FRP plank reinforced beam specimens

a) Gravel coated FRP plank

b) Sand coated FRP plank

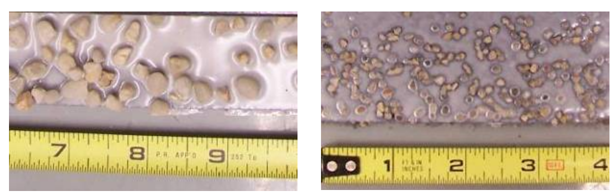

c) Comparison (Left : gravel, Right : sand)

Figure-3 Aggregate coated FRP planks

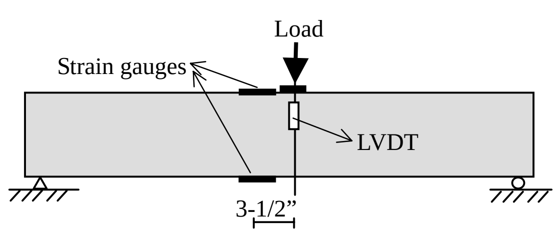

Figure-4 Typical instrumentation for tested specimens

Figure-5 Experiment setup of specimen 1 prior to loading

Figure-6 Experiment setup of specimen 4 prior to loading

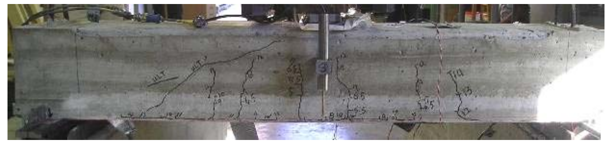

a) Shear failure of specimen 1

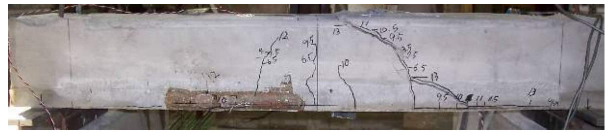

b) Shear failure of specimen 2

c) Shear failure of specimen 3

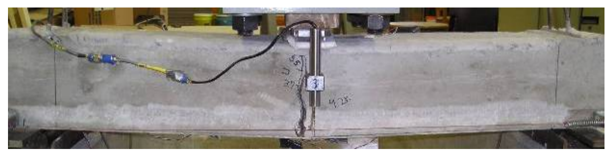

d) Flexural failure of specimen C1

Figure-7 Specimens 1-3 and C1 after test

1) Hybrid failure mode of specimen 4

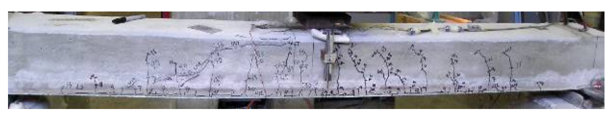

2) Hybrid failure mode of specimen 5

3) Flexural failure of specimen C2

Figure-8 Specimens 4-5 and C2 after test

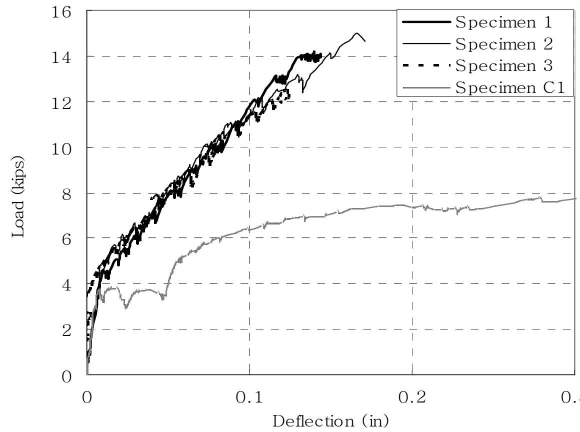

Figure-9 Load-deflection plots for specimens 1-3 and C1

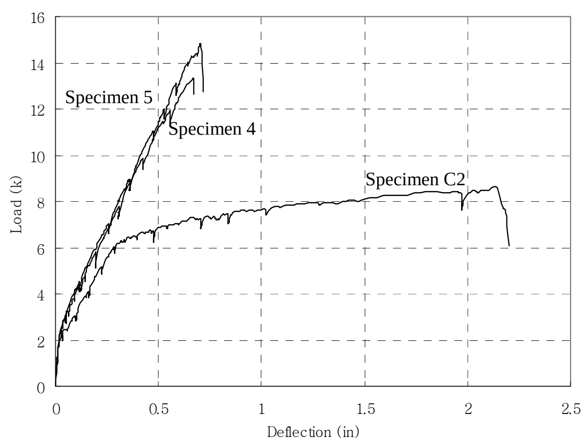

Figure-10 Load-deflection plots for specimens 4-5 and C2

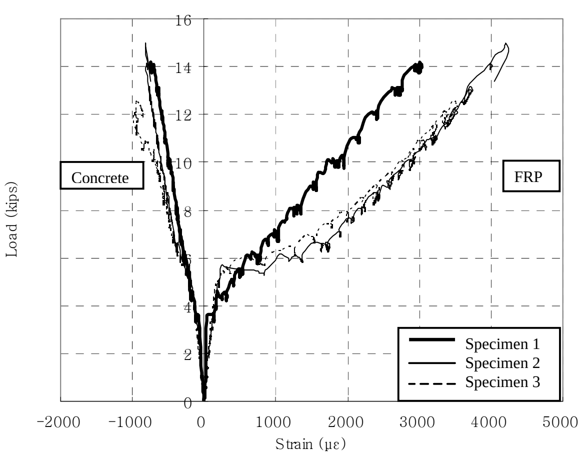

Figure-11 Load-strain plots for specimens 1-3

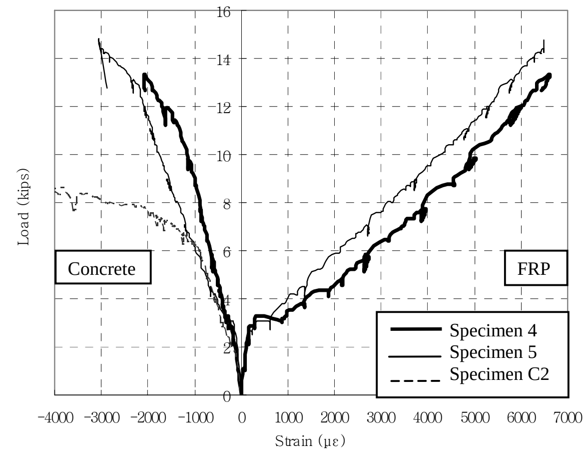

Figure-12 Load-strain plots for specimens 4-5 and C2

Table 1. Details of the fabricated beams

Specimen I.D.	Span	Tensile Reinforcement	Compressive strength (Psi)
1	3'7"	Gravel coated FRP plank	3,740
2	3'7"	Sand coated FRP plank	3,740
3	3'7"	Sand coated FRP plank	3,550
C1*	3'7"	FRP plank	3,740
4	6'	Sand coated FRP plank	4,650
5	6'	Sand coated FRP plank	4,860
C2*	6'	Steel reinforcement (3-#3)	4,775

* Control specimen

Table 2. Test results

Specimen I.D.	Span	Initial cracking load (kips)	Nomalized* initial cracking moment (k-in)	Failure load (kips)	Deflection at failure load (in)	# of flexural cracks at both side	Failure mode
1	3’ 7”	3.5	38.9	14.2	0.140	11	Shear
2	3’ 7”	4.7	52.3	15.0	0.166	9	Shear
3	3’ 7”	5.0	57.1	12.9	0.166	9	Shear
C1	3’ 7”	3.4	37.8	3.8 (9.2**)	0.017	3	Flexural
4	6’	2.8	46.7	13.4	0.669	22	Hybrid
5	6’	2.7	44.1	14.8	0.705	29	Hybrid
C2	6’	1.8	29.7	8.6	2.145	22	Flexural

* Normalized value to concrete with 4,000 psi of compressive strength
** Secondary peak load

Table 2. Test results (continued)

Specimen I.D.	Measured strain at initial cracking load (με)		Measured strain at failure load (με)	
	Concrete (Compression)	FRP (Tension)	Concrete (Compression)	FRP (Tension)
1	-74	37	740	3,000
2	-164	179	812	4,203
3	-180	176	802	3,621
C1	-100	139	187	619
4	-197	151	2,091***	6,610
5	-188	243	3,047	6,496
C2	-112	-	3,804	-

*** Concrete crushing didn’t occurred at the gauge location and it showed less value

Table 3. Comparison of the test results to Code predictions

Specimen I.D.	Initial cracking load (kips)		Failure load (kips)			
	Test	ACI 318	Test	ACI 318 (Shear failure)	ACI 440 (Shear failure)	ACI 440 (Flexural failure*)
1	3.5	2.8	14.2 (Shear failure)	12.7	8.2	24.6
2	4.7	2.8	15.0 (Shear failure)	12.7	8.2	24.6
3	5.0	2.7	12.9 (Shear failure)	12.4	8.1	23.7
C1	3.4	2.8	3.8 (Flexural failure)	-	-	-
4	2.8	1.9	13.4 (Hybrid failure)	14.2	8.7	17.0
5	2.7	1.9	14.8 (Hybrid failure)	14.5	8.8	17.5
C2	1.8	1.9	8.6 (Flexural failure)	11.7	-	5.5

* Calculated with an assumption of full composite action between FRP plank and concrete. For C2 the flexural capacity was calculated using ACI 318